

## Supporting Information

LiO<sub>4</sub> tetrahedra lock alignment of  $\pi$ -conjugated layers to maximize optical anisotropy  
in metal hydroisocyanurates

Xianghe Meng,<sup>a,d,#</sup> Fei Liang,<sup>a,#</sup> Jian Tang,<sup>b,c</sup> Kaijin kang,<sup>b,c</sup> Wenlong Yin,<sup>\*b</sup> Tixian  
Zeng,<sup>c</sup> Bin Kang,<sup>b</sup> Zheshuai Lin,<sup>a</sup> and Mingjun Xia<sup>\*a,d</sup>

<sup>a</sup>Beijing Center for Crystal Research and Development, Key Laboratory of Functional Crystals and Laser Technology, Technical Institute of Physics and Chemistry, Chinese Academy of Sciences, Beijing 100190, China. Email: xiamingjun@mail.ipc.ac.cn.

<sup>b</sup>Institute of Chemical Materials, China Academy of Engineering Physics, Mianyang 621900, China. E-mail: wlyin@caep.cn

<sup>c</sup>Physics and Space Science College, China West Normal University, Nanchong 637002, China

<sup>d</sup>Center of Materials Science and Optoelectronics Engineering, University of Chinese Academy of Sciences, Beijing 100049, China

## Table of Contents

Experimental procedures .....	S3
1. Synthesis .....	S3
2. Powder X-ray diffraction .....	S3
3. UV-vis–NIR diffuse reflectance spectrum .....	S3
4. Infrared spectrum .....	S3
5. Raman spectrum .....	S3
6. Thermal analysis .....	S3
7. Single crystal structure determination .....	S4
8. Computational methods .....	S4
Result and discussion.....	S5
Figure S1. Experimental and calculated XRD patterns for <b>LCHCY</b> and <b>NBHCY</b> .....	S5
Figure S2. UV–vis–NIR diffuse reflectance spectra of <b>LCHCY</b> and <b>NBHCY</b> .....	S6
Figure S3. TG curve of <b>LCHCY</b> .....	S7
Figure S4. IR spectrum of <b>LCHCY</b> .....	S8
Figure S5. Raman spectrum of <b>LCHCY</b> .....	S9
Figure S6. Band structures of (a) <b>LCHCY</b> and (b) <b>NBHCY</b> .....	S10
Figure S7. The partial density of states projected constituent atoms of (a) <b>LCHCY</b> and (b) <b>NBHCY</b> (The contribution from H <sub>2</sub> O molecule was omitted for simplification).....	S11
Figure S8. The refractive dispersion curves of <b>NBHCY</b> .....	S12
Table S1. Crystal data and structure refinement for <b>LCHCY</b> and <b>NBHCY</b> .....	S13
Table S2. Atomic coordinates and equivalent isotropic displacement parameters (Å <sup>2</sup> ) for <b>LCHCY</b> .....	S14
Table S3. Atomic coordinates and equivalent isotropic displacement parameters (Å <sup>2</sup> ) for <b>NBHCY</b> .....	S15
Table S4. Selected bond lengths (Å) and bond angles (degree) for <b>LCHCY</b> .....	S16
Table S5. Selected bond lengths (Å) and bond angles (degree) for <b>NBHCY</b> .....	S17
References.....	S18

## **Experimental procedures**

### **1. Synthesis**

All chemicals containing LiOH·H<sub>2</sub>O (98%, Aladdin), NaOH (98%, Aladdin), Ca(OH)<sub>2</sub> (98%, Aladdin), Ba(OH)<sub>2</sub>·8H<sub>2</sub>O (99%, Alfa Aesar) and H<sub>3</sub>C<sub>3</sub>N<sub>3</sub>O<sub>3</sub> (98%, Aladdin) were used without further purification. **LCHCY/NBHCY** crystals were grown by dissolving LiOH·H<sub>2</sub>O/NaOH (2 mmol), Ca(OH)<sub>2</sub>/Ba(OH)<sub>2</sub>·8H<sub>2</sub>O (1 mmol) and H<sub>3</sub>C<sub>3</sub>N<sub>3</sub>O<sub>3</sub> (4 mmol) in 30 mL of demineralized water in a clean beaker with stirring and heating using magnetic stirrer at the boiling point until the solution was concentrated to 15 mL. Then the beaker was put in the open air to cool down naturally. Colorless crystals were obtained after cooling down to room temperature.

### **2. Powder X-ray diffraction**

The powder X-ray diffraction (PXRD) data were collected on Bruker D8 Focus diffractometer equipped with Cu K $\alpha$  radiation ( $\lambda=1.5418\text{ \AA}$ ) in the  $2\theta$  range of 5-70° at room temperature.

### **3. UV-vis-NIR diffuse reflectance spectrum**

The UV–vis–NIR diffuse reflectance spectra were measured in the wavelength range from 200 nm to 1400 nm with BaSO<sub>4</sub> as a reference material by Cary 7000 UV-vis-NIR universal measurement spectrophotometer under an integrating sphere.

### **4. Infrared spectrum**

Infrared spectroscopy was collected on a Varian Excalibur 3100 spectrometer in the 400 - 3600 cm<sup>-1</sup> range. **LCHCY** and KBr samples were mixed thoroughly with mass ratio about 1:100, respectively.

### **5. Raman spectrum**

Raman spectra were measured using an InVia Raman spectrometer (Renishaw, Inc.) with exciting wavelength at 532 nm in the 50 - 2000 cm<sup>-1</sup> range at room temperature.

### **6. Thermal analysis**

Thermal gravimetric (TG) analysis were carried out on NETZSCH STA 409 CD thermal analyzer in the temperature range of 50-600 °C for **LCHCY** with a heating rate of 10 K/min under nitrogen atmosphere.

## 7. Single crystal structure determination

The single-crystal X-ray diffraction data was gathered on a Rigaku AFC10 single-crystal diffractometer equipped with graphite-monochromatic Mo K $\alpha$  radiation ( $\lambda=0.71073\text{ \AA}$ ) and Saturn CCD detector at 293 K. The intensity data, data reduction and cell refinement were captured by the CrystalClear program. The crystal structures were settled by the direct method with program SHELXS-97 and further refined by full matrix least squares on  $F^2$  by SHELXL-97 programs. The structure was confirmed by the ADDSYM algorithm from the program PLATON with no higher symmetry discovered. The crystallographic data are given in Table S1 - S5.

## 8. Computational methods

The theoretical simulations for **LCHCY** and **NBHCY** were performed by first principles density functional theory<sup>1</sup> from CASTEP module,<sup>2</sup> which has been utilized on metal cyanurates and hydrocyanurates successfully.<sup>3-7</sup> The exchange–correlation (XC) functional was modeled by the generalized gradient density approximation (GGA)<sup>8</sup> and the norm-conserving pseudopotentials<sup>9</sup> were applied for all elements. In this model, Li 2s, Na 2p<sup>6</sup>3s, Ba 5p<sup>6</sup>6s<sup>2</sup>, Ca 3p<sup>6</sup>4s<sup>2</sup>, C 2s<sup>2</sup>2p<sup>2</sup>, N 2s<sup>2</sup>2p<sup>3</sup>, O 2s<sup>2</sup>2p<sup>4</sup> and H 1s electrons were modeled as the outer valence electrons, respectively. The kinetic energy cutoff of 770 eV and dense  $k$ -point meshes<sup>10</sup> (4×4×5 for **LCHCY** and 2×2×4 for **NBHCY**) in the first Brillouin zone were chosen to guarantee the sufficient calculation accuracy. In order to elaborate the origin of large birefringence in **LCHCY**, the optical properties of two isostructural compounds, K<sub>2</sub>(HC<sub>3</sub>N<sub>3</sub>O<sub>3</sub>)<sup>11</sup>, were also calculated for comparison.

## Result and discussion

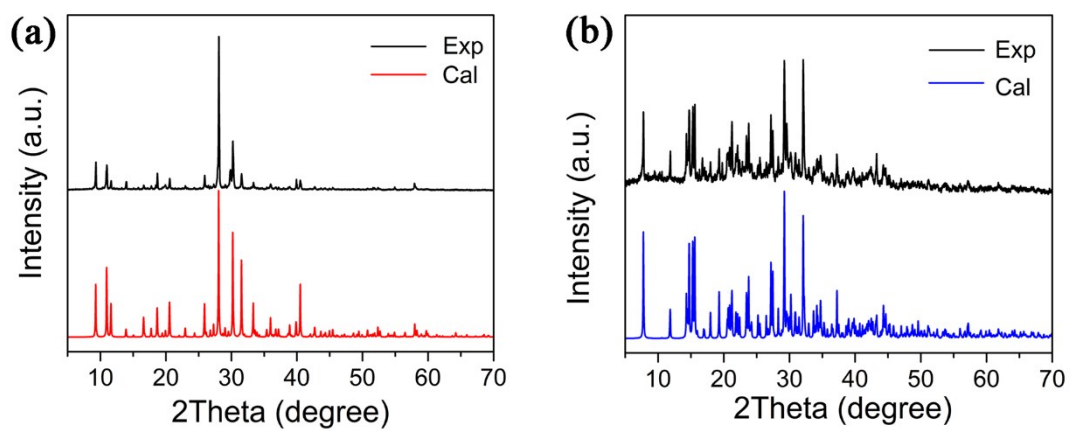


Figure S1. Experimental and calculated XRD patterns for **LCHCY** and **NBHCY**.

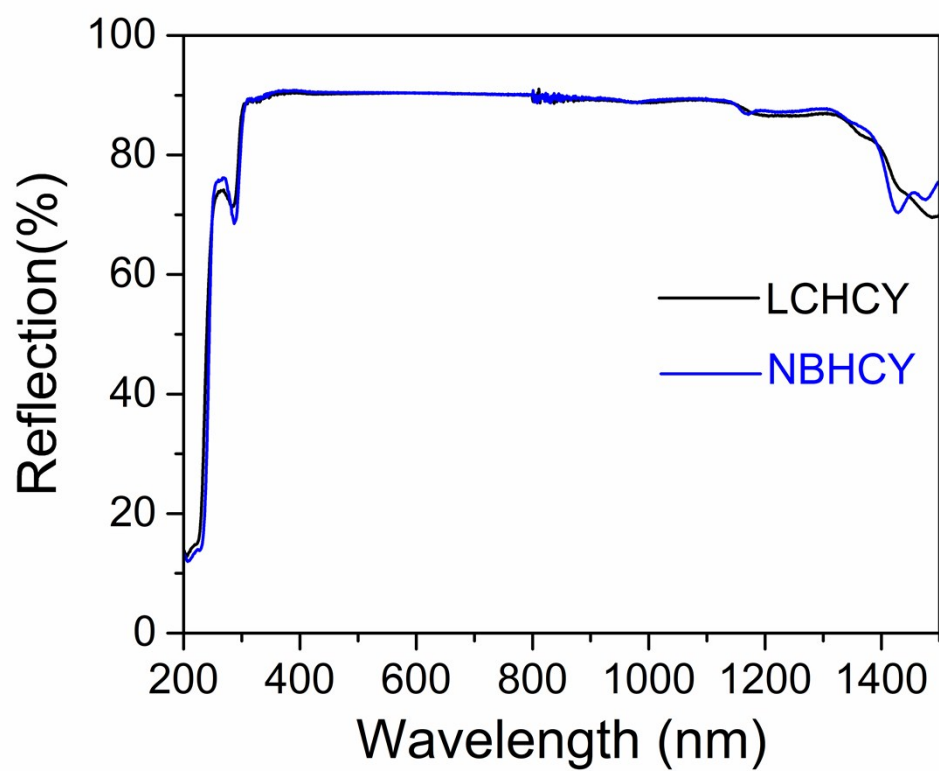


Figure S2. UV–vis–NIR diffuse reflectance spectra of **LCHCY** and **NBHCY**.

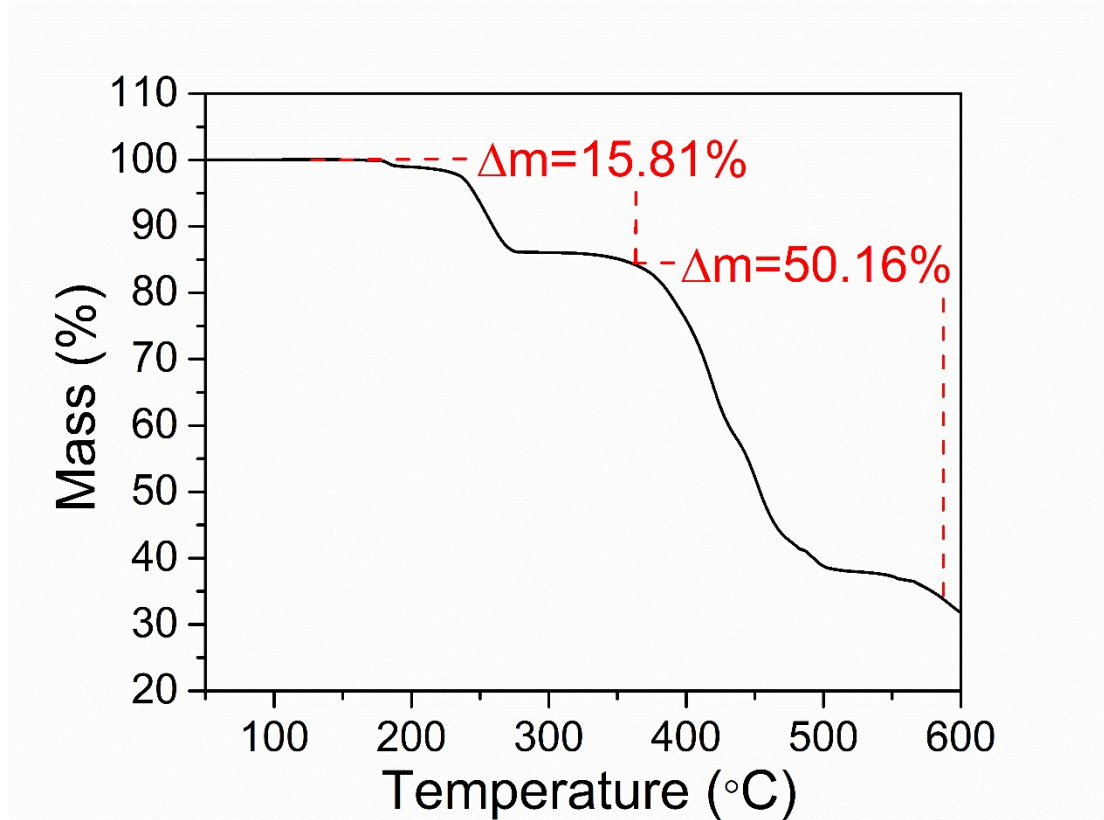


Figure S3. TG curve of LCHCY.

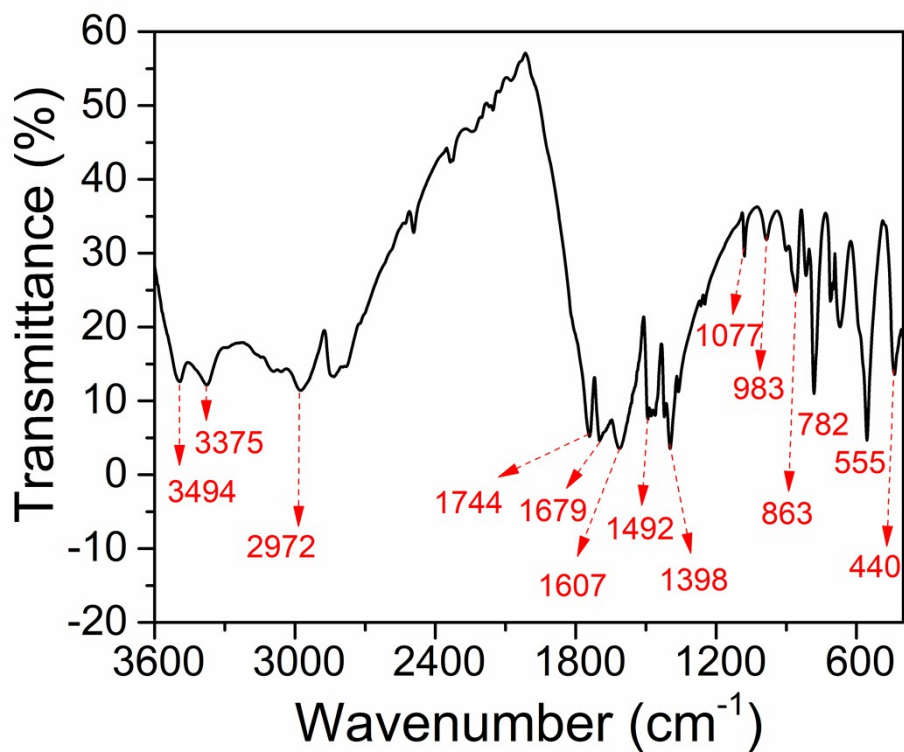


Figure S4. IR spectrum of LCHCY.

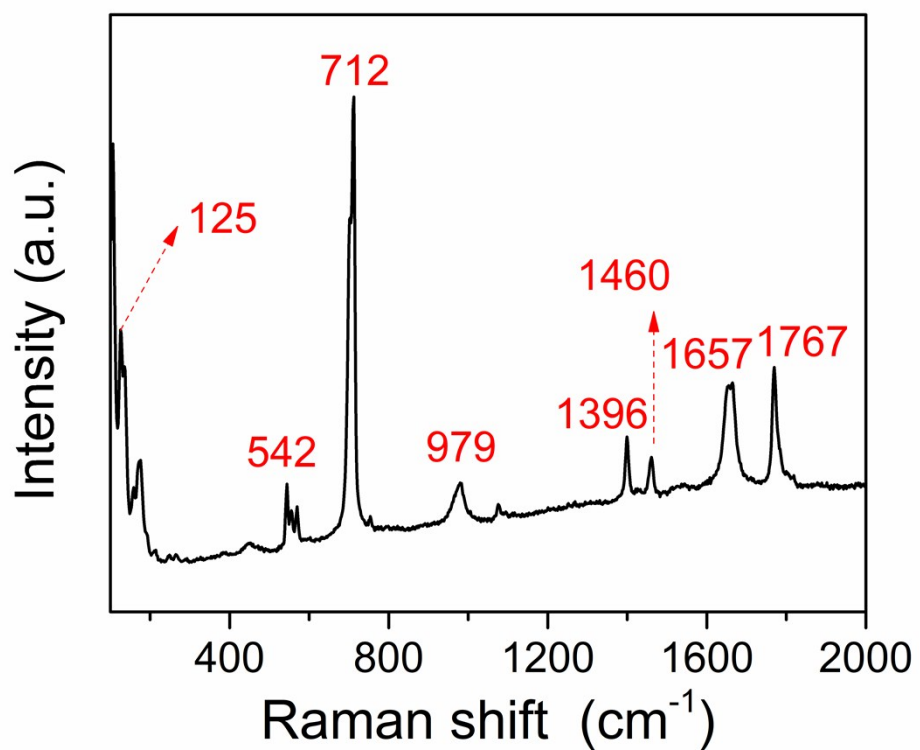


Figure S5. Raman spectrum of LCHCY.

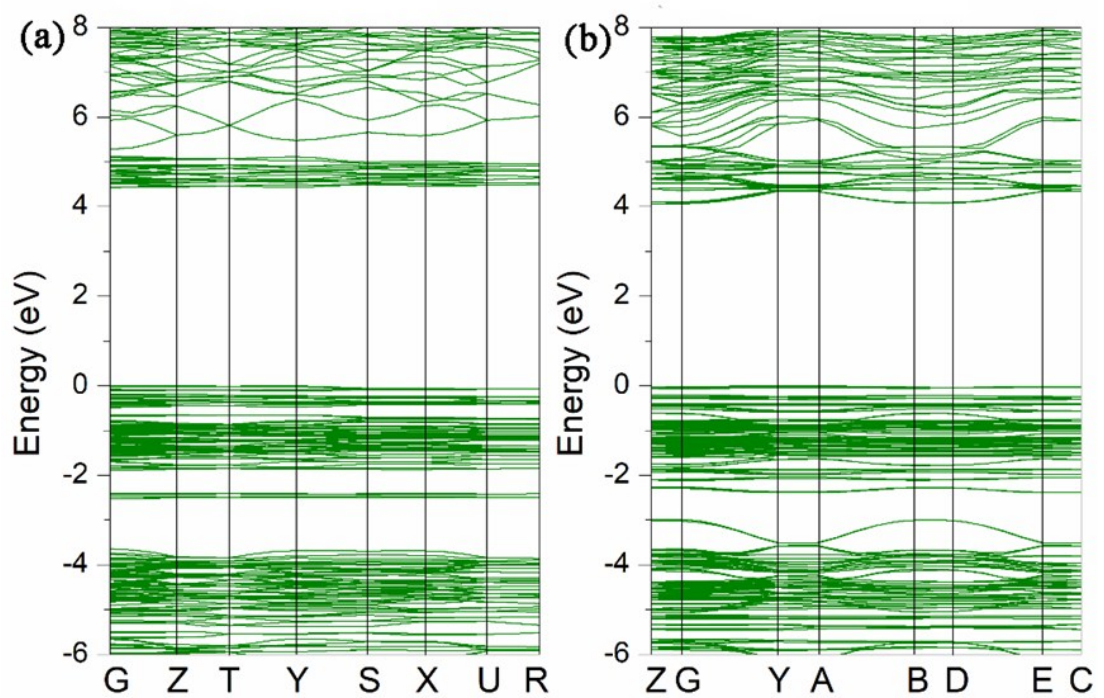


Figure S6. Band structures of (a) **LCHCY** and (b) **NBHCY**.

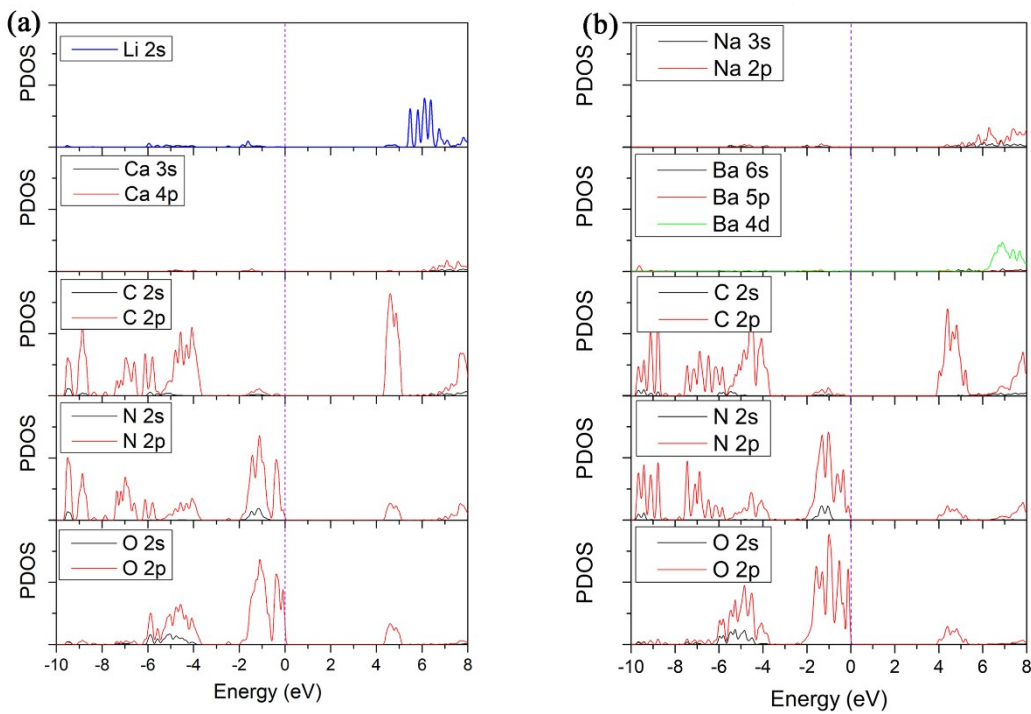


Figure S7. The partial density of states projected constituent atoms of (a) **LCHCY** and (b) **NBHCY** (The contribution from H<sub>2</sub>O molecule was omitted for simplification).

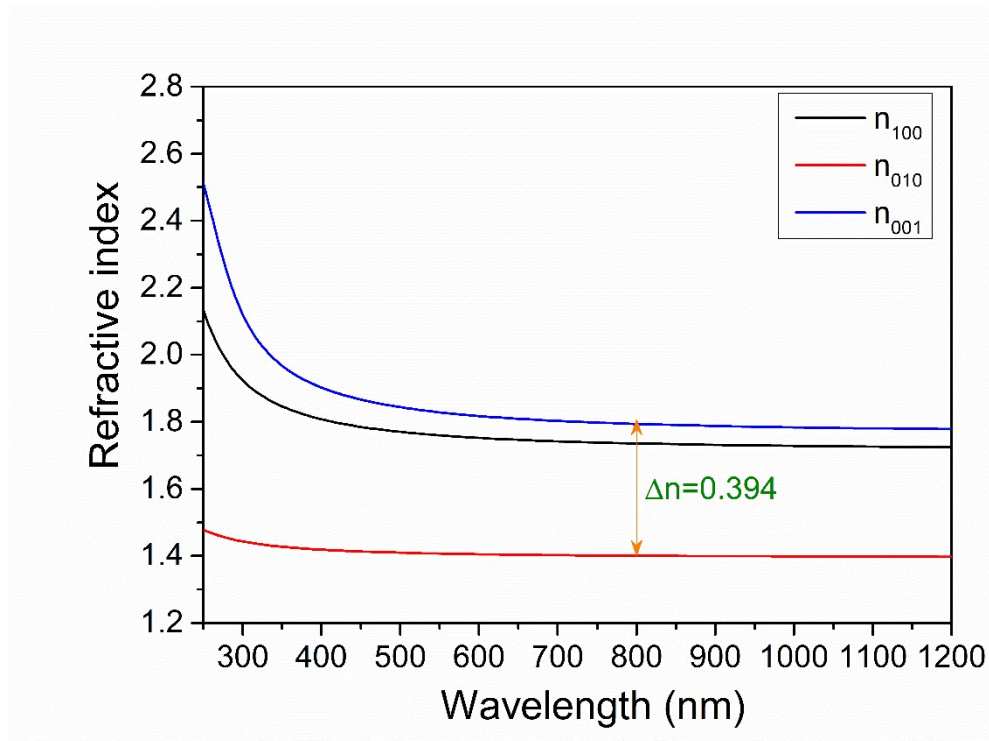


Figure S8. The refractive dispersion curves of **NBHCY**.

Table S1. Crystal data and structure refinement for **LCHCY** and **NBHCY**.

Formula	$\text{Li}_2\text{Ca}(\text{H}_2\text{C}_3\text{N}_3\text{O}_3)_4 \cdot 6\text{H}_2\text{O}$	$\text{Na}_2\text{Ba}(\text{H}_2\text{C}_3\text{N}_3\text{O}_3)_4 \cdot 6\text{H}_2\text{O}$
Formula weight(g/mol)	674.36	803.72
Temperature/K	293	293
Crystal system	orthorhombic	monoclinic
Space group	<i>C</i> mcm	<i>C</i> 2/c
a/Å	16.1096(10)	17.0294(6)
b/Å	11.7548(6)	6.5546(2)
c/Å	12.7052(9)	23.1652(8)
$\alpha/^\circ$	90	90
$\beta/^\circ$	90	101.245(3)
$\gamma/^\circ$	90	90
Volume/Å <sup>3</sup>	2405.9(3)	2536.08(15)
Z	4	4
$\rho_{\text{calc}}/\text{g/cm}^3$	1.862	2.105
$\mu/\text{mm}^{-1}$	0.377	1.712
F(000)	1384	1592.0
Radiation	Mo K $\alpha$ ( $\lambda = 0.71073$ )	Mo K $\alpha$ ( $\lambda = 0.71073$ )
Independent reflections	1334 [ $R_{\text{int}} = 0.0534$ ]	2599 [ $R_{\text{int}} = 0.0295$ ]
Goodness-of-fit on $F^2$	1.046	1.090
Final R indexes [I $\geq 2\sigma$ (I)]	$R_1 = 0.0355$ , $wR_2 = 0.1013$	$R_1 = 0.0183$ , $wR_2 = 0.0453$
Final R indexes [all data]	$R_1 = 0.0431$ , $wR_2 = 0.1068$	$R_1 = 0.0188$ , $wR_2 = 0.0456$

Table S2. Atomic coordinates and equivalent isotropic displacement parameters ( $\text{\AA}^2$ ) for **LCHCY**.

<b>LCHCY</b>				
Atom	x	y	z	U(eq)
Ca1	0.5000	0.71839 (6)	0.7500	0.0253 (2)
Li1	0.5000	0.1827 (5)	0.7500	0.0315 (13)
Li2	0.5000	0.4301 (5)	0.7500	0.0370 (15)
O1	0.14538 (10)	-0.06612 (13)	0.7500	0.0262 (4)
O2	0.15127 (10)	0.31675 (14)	0.7500	0.0315 (4)
O3	0.39261 (11)	0.11658 (15)	0.7500	0.0378 (5)
O4	0.10890 (11)	0.5000	0.5000	0.0399 (5)
O5	0.35154 (7)	0.30758 (9)	0.51355 (11)	0.0293 (3)
O6	0.5000	0.29623 (15)	0.63401 (15)	0.0301 (4)
O7	0.5000	0.55559 (14)	0.62993 (14)	0.0261 (4)
O8	0.5000	0.84410 (18)	0.89344 (19)	0.0454 (6)
N1	0.14383 (11)	0.12676 (16)	0.7500	0.0228 (4)
N2	0.26899 (11)	0.02506 (16)	0.7500	0.0227 (4)
N3	0.27370 (12)	0.22029 (16)	0.7500	0.0240 (5)
N4	0.23051 (8)	0.40273 (11)	0.50494 (11)	0.0242 (4)
N5	0.35836 (11)	0.5000	0.5000	0.0229 (4)
C1	0.18327 (14)	0.02641 (19)	0.7500	0.0195 (5)
C2	0.18803 (14)	0.22310 (19)	0.7500	0.0215 (5)
C3	0.31735 (15)	0.1208 (2)	0.7500	0.0236 (5)
C4	0.18434 (15)	0.5000	0.5000	0.0243 (5)
C5	0.31604 (10)	0.40134 (13)	0.50685 (13)	0.0213 (4)

Table S3. Atomic coordinates and equivalent isotropic displacement parameters ( $\text{\AA}^2$ ) for **NBHCY**.

Atom	x	y	z	U(eq)
Ba1	0.5000	0.30296 (2)	0.7500	0.02101 (6)
Na1	0.51333 (5)	0.48259 (14)	0.57942 (4)	0.03295 (19)
C1	0.17847 (11)	0.5058 (3)	0.47514 (8)	0.0222 (4)
C2	0.69355 (11)	0.4306 (3)	0.75666 (8)	0.0224 (4)
C3	0.81927 (11)	0.4483 (3)	0.72422 (8)	0.0223 (4)
C4	0.69103 (11)	0.4430 (3)	0.65701 (8)	0.0225 (4)
C5	0.30432 (11)	0.4853 (3)	0.54415 (9)	0.0245 (4)
C6	0.17650 (11)	0.4770 (3)	0.57470 (8)	0.0227 (4)
N1	0.26106 (9)	0.5031 (3)	0.48840 (7)	0.0240 (3)
N2	0.13688 (9)	0.4941 (3)	0.51875 (7)	0.0236 (3)
N3	0.77445 (9)	0.4467 (3)	0.66915 (7)	0.0259 (4)
N4	0.65164 (9)	0.4305 (3)	0.70169 (7)	0.0240 (3)
N5	0.77632 (9)	0.4402 (3)	0.76774 (7)	0.0232 (3)
N6	0.25898 (9)	0.4717 (3)	0.58625 (7)	0.0267 (4)
O1	0.65940 (8)	0.4208 (3)	0.79960 (6)	0.0320 (3)
O2	0.89301 (8)	0.4568 (2)	0.73433 (6)	0.0285 (3)
O3	0.49934 (9)	0.1558 (2)	0.63571 (7)	0.0301 (3)
O4	0.49946 (9)	0.7351 (2)	0.50644 (8)	0.0327 (3)
O5	0.14509 (8)	0.5207 (3)	0.42272 (6)	0.0322 (3)
O6	0.65657 (8)	0.4525 (2)	0.60495 (6)	0.0305 (3)
O7	0.49380 (11)	0.6557 (3)	0.67521 (9)	0.0435 (4)
O8	0.14158 (8)	0.4638 (2)	0.61689 (6)	0.0303 (3)
O9	0.37685 (8)	0.4793 (3)	0.55520 (7)	0.0390 (4)

Table S4. Selected bond lengths ( $\text{\AA}$ ) and bond angles (degree) for **LCHCY**.

<b>LCHCY</b>			
Ca1—O8	2.346 (2)	Li2—O1 <sup>iii</sup>	2.3424 (16)
Ca1—O8 <sup>i</sup>	2.346 (2)	O1—C1	1.247 (3)
Ca1—O7	2.4473 (17)	O2—C2	1.250 (3)
Ca1—O7 <sup>i</sup>	2.4473 (17)	O3—C3	1.213 (3)
Ca1—N1 <sup>ii</sup>	2.5551 (19)	O4—C4	1.215 (3)
Ca1—N1 <sup>iii</sup>	2.5551 (19)	O5—C5	1.245 (2)
Ca1—O2 <sup>ii</sup>	2.6972 (17)	N1—C2	1.338 (3)
Ca1—O2 <sup>iii</sup>	2.6972 (17)	N1—C1	1.340 (3)
Li1—O3	1.897 (3)	N2—C3	1.369 (3)
Li1—O3 <sup>iv</sup>	1.897 (3)	N2—C1	1.381 (3)
Li1—O6 <sup>j</sup>	1.988 (4)	N3—C3	1.364 (3)
Li1—O6	1.988 (4)	N3—C2	1.380 (3)
Li2—O7 <sup>i</sup>	2.122 (4)	N4—C4	1.3654 (19)
Li2—O7	2.122 (4)	N4—C5	1.378 (2)
Li2—O6	2.156 (5)	N5—C5	1.3481 (19)
Li2—O6 <sup>j</sup>	2.156 (5)	N5—C5 <sup>vi</sup>	1.3481 (19)
Li2—O1 <sup>ii</sup>	2.3424 (16)	C4—N4 <sup>vi</sup>	1.3654 (19)
C2—N1—C1	119.5 (2)	N1—C2—N3	120.8 (2)
C3—N2—C1	124.0 (2)	O3—C3—N3	123.4 (2)
C3—N3—C2	122.39 (19)	O3—C3—N2	122.3 (2)
C4—N4—C5	123.74 (15)	N3—C3—N2	114.3 (2)
C5—N5—C5 <sup>vi</sup>	119.2 (2)	O4—C4—N4 <sup>vi</sup>	123.01 (10)
O1—C1—N1	122.4 (2)	O4—C4—N4	123.01 (10)
O1—C1—N2	118.6 (2)	N4 <sup>vi</sup> —C4—N4	114.0 (2)
N1—C1—N2	119.0 (2)	O5—C5—N5	122.27 (16)
O2—C2—N1	119.6 (2)	O5—C5—N4	118.11 (15)
O2—C2—N3	119.7 (2)	N5—C5—N4	119.62 (15)

Symmetry codes: (i)  $x, y, -z+3/2$ ; (ii)  $-x+1/2, y+1/2, -z+3/2$ ; (iii)  $x+1/2, y+1/2, z$ ; (iv)  $-x+1, y, -z+3/2$ ; (v)  $x-1/2, y-1/2, z$ ; (vi)  $x, -y+1, -z+1$ .

Table S5. Selected bond lengths ( $\text{\AA}$ ) and bond angles (degree) for **NBHCY**.

Ba1—O3	2.8157 (15)	C1—N2	1.344 (2)
Ba1—O <sub>3</sub> <sup>i</sup>	2.8157 (15)	C1—N1	1.380 (2)
Ba1—O <sub>1</sub> <sup>i</sup>	2.8406 (13)	C2—O1	1.248 (2)
Ba1—O1	2.8406 (14)	C2—N4	1.333 (2)
Ba1—O7	2.8788 (18)	C2—N5	1.384 (2)
Ba1—O <sub>7</sub> <sup>i</sup>	2.8788 (18)	C3—O2	1.233 (2)
Ba1—O <sub>2</sub> <sup>ii</sup>	2.8881 (15)	C3—N3	1.353 (2)
Ba1—O <sub>2</sub> <sup>iii</sup>	2.8881 (14)	C3—N5	1.357 (2)
Ba1—N4	3.1220 (15)	C4—O6	1.236 (2)
Ba1—N <sub>4</sub> <sup>i</sup>	3.1220 (15)	C4—N4	1.341 (2)
Na1—O9	2.2822 (16)	C4—N3	1.393 (2)
Na1—O4	2.3446 (18)	C5—O9	1.212 (2)
Na1—O6	2.4034 (15)	C5—N6	1.360 (2)
Na1—O <sub>4</sub> <sup>iv</sup>	2.4228 (19)	C5—N1	1.361 (2)
Na1—O3	2.5430 (18)	C6—O8	1.242 (2)
Na1—O7	2.571 (2)	C6—N2	1.344 (2)
C1—O5	1.240 (2)	C6—N6	1.378 (2)
O5—C1—N2	122.16 (17)	O9—C5—N1	122.94 (18)
O5—C1—N1	118.14 (16)	N6—C5—N1	114.09 (16)
N2—C1—N1	119.70 (17)	O8—C6—N2	122.50 (17)
O1—C2—N4	121.04 (16)	O8—C6—N6	118.14 (17)
O1—C2—N5	118.07 (17)	N2—C6—N6	119.36 (16)
N4—C2—N5	120.89 (16)	C5—N1—C1	123.49 (16)
O2—C3—N3	123.07 (17)	C6—N2—C1	119.38 (16)
O2—C3—N5	122.50 (17)	C3—N3—C4	123.77 (16)
N3—C3—N5	114.43 (16)	C2—N4—C4	118.82 (16)
O6—C4—N4	122.85 (17)	C4—N4—Ba1	150.01 (12)
O6—C4—N3	117.88 (16)	C3—N5—C2	122.75 (16)
N4—C4—N3	119.26 (16)	C5—N6—C6	123.97 (16)
O9—C5—N6	122.97 (18)		

Symmetry codes: (i)  $-x+1, y, -z+3/2$ ; (ii)  $x-1/2, y-1/2, z$ ; (iii)  $-x+3/2, y-1/2, -z+3/2$ ; (iv)  $-x+1, -y+1, -z+1$ ; (v)  $x+1/2, y+1/2, z$ .

## References

- (1) Kohn, W. Nobel Lecture: Electronic structure of matter-wave functions and density functionals. *Rev. Mod. Phys.* **1999**, *71*, 1253-1266.
- (2) Clark, S. J.; Segall, M. D.; Pickard, C. J.; Hasnip, P. J.; Probert, M. J.; Refson, K.; Payne, M. C. First Principles Methods Using CASTEP. *Z. Kristallogr.* **2005**, *220*, 567-570.
- (3) Liang, F.; Kang, L.; Zhang, X.; Lee, M.; Lin, Z.; Wu, Y. Molecular Construction Using  $(C_3N_3O_3)^{3-}$ -Anions: Analysis and Prospect for Inorganic Metal Cyanurates Nonlinear Optical Materials. *Cryst. Growth & Des.* **2017**, *17*, 4015-4020.
- (4) Li, Z.; Liang, F.; Guo, Y.; Lin, Z.; Yao, J.; Zhang, G.; Yin, W.; Wu, Y.; Chen, C.  $Ba_2M(C_3N_3O_3)_2$  ( $M = Mg, Ca$ ): Potential UV Birefringent Materials with Strengthened Optical Anisotropy Originating from the  $(C_3N_3O_3)^{3-}$  Group. *J. Mater. Chem. C* **2018**, *6*, 12879-12887.
- (5) Xia, M.; Zhou, M.; Liang, F.; Meng, X.; Yao, J.; Lin, Z.; Li, R. Noncentrosymmetric Cubic Cyanurate  $K_6Cd_3(C_3N_3O_3)_4$  Containing Isolated Planar  $\pi$ -Conjugated  $(C_3N_3O_3)^{3-}$  Groups. *Inorg. Chem.* **2018**, *57*, 32-36.
- (6) Tang, J.; Liang, F.; Meng, X.; Kang, K.; Yin, W.; Zeng, T.; Xia, M.; Lin, Z.; Yao, J.; Zhang, G.; Kang, B.  $Ba_3(C_3N_3O_3)_2$ : A New Phase of Barium Cyanurate Containing Parallel  $\pi$ -Conjugated Groups as a Birefringent Material Replacement for Calcite. *Cryst. Growth & Des.* **2019**, *19*, 568-572.
- (7) Wang, N.; Liang, F.; Yang, Y.; Zhang, S.; Lin, Z. A New Ultraviolet Transparent Hydra-cyanurate  $K_2(C_3N_3O_3H)$  with Strong Optical Anisotropy from Delocalized  $\pi$ -bonds. *Dalton Trans.* **2019**, *48*, 2271-2274.
- (8) Perdew, J. P.; Burke, K.; Ernzerhof, M. Generalized Gradient Approximation Made Simple. *Phys. Rev. Lett.* **1996**, *77*, 3865-3868.
- (9) Vanderbilt, D. Soft Self-consistent Pseudopotentials in a Generalized Eigenvalue Formalism. *Phys. Rev. B* **1990**, *41*, 7892-7895.
- (10) Monkhorst, H. J.; Pack, J. D. Special Points For Brillouin-Zone Integrations. *Phys. Rev. B* **1976**, *13*, 5188-5192.
- (11) Nichol, G. S.; Clegg, W.; Gutmann, M. J.; Tooke, D. M. Stoichiometry-dependent Structures: an X-ray and Neutron Single-crystal Diffraction Study of the Effect of Reaction Stoichiometry on the Crystalline Products Formed in the Potassium-cyanurate System. *Acta crystallographica. Section B, Structural science* **2006**, *62*, 798-807.